

Accuracy Enhancements for TDOA Estimation on Highly Resource Constrained Mobile Platforms

Kumar Gaurav Chhokra¹, Theodore Bapty¹, Jason Scott¹, Mitch Wilkes²

¹Institute for Software Integrated Systems, Vanderbilt University

{kumar, bapty, jscott}@isis-server.isis.vanderbilt.edu

Tel: (615) 343 7567, Fax: (615) 343 7440

²Electrical Engineering and Computer Science, Vanderbilt University

{mitch.wilkes@vanderbilt.edu}

Abstract.

Over the past few years, there has been an immense thrust in the field of geolocation, surveillance, tracking and location-aware systems and services. The advent of compact, low power, high-processing power DSPs have made possible several tasks which were infeasible just a few years ago. TDOA estimates on such energy and resource constrained platforms suffers from the lack of a coherent sampling clock. We present two related techniques of Doppler-frequency and time shift correction. The techniques are formally developed, analyzed. They are then compared from an implementation and performance perspective.

1. Introduction

Over the past few years, there has been an immense thrust in the field of geolocation, surveillance, tracking and location-aware systems and services. The advent of compact, low power, high-processing power digital signal processors have made possible several tasks which were considered infeasible just a few years ago. The applications abound in utilitarian (E911, product-customized services, in-building tracking, etc.) and military sectors (surveillance, un-manned reconnaissance, target location etc.) [1-4].

Traditional TDOA / TOA systems used for geolocation depend heavily on fixed array based processing and typically employ high precision, costly components. Such systems also have long stand off ranges, making it difficult to closely track and follow the movements of targets with low power signals and in congested areas [5]. Proximity to target and mobility of the tracking devices gathers greater relevance in urban environments.

Unmanned aerial vehicles (UAVs) and organic aerial vehicles (OAVs) equipped with geolocation electronics can counter the problems with long-standoff systems. They can afford safety, security and stealth for the reconnaissance mission. However, they pose interesting technical constraints. Robustness and reliability under military use conditions demand that the devices be compact, rugged and mechanically stable. Stealth in reconnaissance implies a small, silent design (i.e. limited communication bandwidth) while, endurance and usability demand an extensive operating life (i.e. low power). These UAVs are imagined as a fleet of dispensable mobile devices, implying a relatively

strong constraint on the manufacturing and operating cost.

These real-world constraints manifest themselves in the algorithmic and signal processing domain as well. Physically distinct, passive RF and mobile units imply the lack of a common clock, thus obviating array based processing. Stealth prevents the UAVs from synchronizing on a regular basis to maintain a common clock, complicating accurate TOA estimates. Also, a reduced communication bandwidth between the devices negates the usual techniques of correlating received signals for TDOA estimates.

These constraints suggest a technique where much of the detection, identification and TOA are done locally and the actual target locus computation is relegated to a remote base station with bandwidth-constrained inputs from the individual UAV sensors. Specifically, each UAV must compute absolute TOA using *a-priori* information such as a signal template, (known signal features, synchronization sequences, etc). TOA processing must then compensate for relatively low precision GPS clocks and unique (possibly varying) sample rates at the sensors.

This paper[‡] describes two techniques for correcting the errors in TOA/TDOA estimates due to incongruent sampling frequencies of the received and template signals. Section II introduces and models the effects of disparate sampling frequencies as a relative time companding (RTC) problem mathematically. Section III introduces the Doppler shift correction technique for narrow band signals. Section IV explains the motivation for a time domain correction. Section V develops the

[‡] This work has been supported by DARPA under the WASP contract F30602-02-2-0206

time-shift correction technique. Section VI compares and contrasts the two techniques with respect to performance characteristics and computational efficiency with field data.

2. Mathematical preliminaries

A signal emanating from a remote source and monitored in the presence of noise at two spatially separate sensors may be mathematically modeled as:

$$x_1(t) = f(t) + n_1(t) \quad (1a)$$

$$x_2(t) = mf(t + D) + n_2(t) \quad (1b)$$

where $f(t)$, $n_1(t)$ and $n_2(t)$ are real, jointly stationary random processes. The signal $f(t)$ is assumed to be uncorrelated with noise $n_1(t)$ and $n_2(t)$. D is the delay between the two received signals.

The traditional technique of detecting a signal of interest (template) buried in a data stream corrupted by additive Gaussian random noise is to use a matched filter or a generalized cross correlator (GCC) [6]. Since the GCC approach may be viewed as pre-filtering the two signals with whitening filters before a usual cross-correlation, we focus on the correlation technique for simplicity. The correlation function may be written as [7]:

$$Rx_1x_2(\tau) = \int_{-\infty}^{\infty} x_1(t)x_2(t + \tau)dt \quad (2)$$

The value of τ that maximizes (2) provides an estimate of the delay D .

2.1. Scaling due to disparate sampling frequencies

Since the signal processing components on the UAVs are subjected to a wide gamut of operating conditions, the operating clock and sampling frequencies are seldom the same as those in the test environments. In particular, the frequency at which the template was constructed is generally different from the frequency at which the incoming signal is sampled. [8] and [9] provide a good discussion of the effects of RTC on the cross-correlation operation. [10] extends the argument to quadratic delays.

Fig. 1 illustrates the effects of different sampling frequencies. The signal with a nominal Fourier transform is sampled at two sampling frequencies, f_{s1} and f_{s2} , with $f_{s1} < f_{s2}$. The sampled signal has different normalized bandwidths given by (3) where $\omega_{si} = 2\pi f_{si}$.

$$\hat{\omega}_{b1} = \frac{\omega_b}{\omega_{s1}} \quad \text{and} \quad \hat{\omega}_{b2} = \frac{\omega_b}{\omega_{s2}} \quad (3)$$

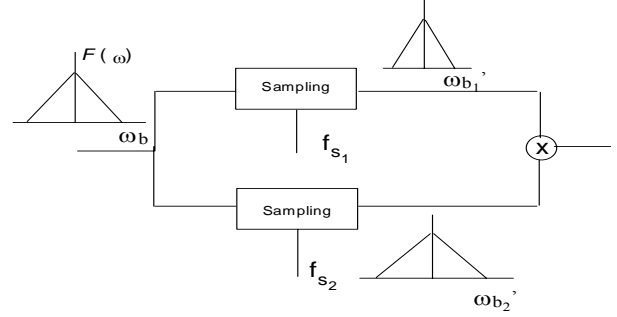


Figure 1 different sampling frequencies lead to frequency companding

Clearly the higher sampling frequency produces a smaller normalized bandwidth, i.e., $\omega_{b2} < \omega_{b1}$. When viewed in the time domain, the differing relative bandwidths manifest themselves as time scaling artifacts.

3. Time scaling and Doppler shift

The disparate sampling frequencies of the template and the UAVs produce correlation artifacts, leading to erroneous time delay and TOA estimates. For relatively narrow-band signals and fairly similar sampling frequencies, it is now shown that the RTC between the template and received signal may be approximated by Doppler shifts. Weiss [11] gives a good explanation of the narrow band criterion. The signals under consideration fall well within the domain of narrow band representation.

Let the template be represented by $f(t)$ and the received signal by $g(t)$. Both signals are considered to be real and continuous as this eases analysis.

Let the received signal suffer both a scaling, given by the scale parameter s , and a time delay, τ :

$$g(t) = f(s(t - \tau)) \quad (4)$$

Taking the Fourier transform on both sides, we have,

$$G(\omega) = s^{-1}F(\omega/s)e^{-j\omega\tau} \quad (5)$$

Let $s = 1 - a$, then

$$G(\omega) = 1/(1 - a)F(\omega/(1 - a))e^{-j\omega(1 - a)\tau} \quad (6)$$

$$\text{if } a \ll 1, \text{ we have } \frac{1}{1 - a} \approx 1 + a \quad (7)$$

$$G(\omega) = (1 + a)F(\omega(1 + a))e^{-j\omega(1 - a)\tau} \quad (8)$$

For narrow band signals,

$$F(\omega_0 + \delta\omega) = 0, |\delta\omega| > \frac{\omega_b}{2} \quad (9)$$

where ω_0 is the center radian frequency and ω_b is the bandwidth of the signal. Hence the above expression for $G(\omega)$ may be approximated by:

$$G(\omega) \approx (1+a)F(\omega+a\omega_0)e^{-j\omega\tau}e^{j\omega a\tau} \quad (10)$$

Noting that both a and τ are small, so that the second exponential maybe approximated by unity, we get,

$$G(\omega) \approx (1+a)F(\omega+a\omega_0)e^{-j\omega\tau} \quad (11)$$

Taking the inverse Fourier transform, we obtain,

$$g(t) \approx f(t-\tau)e^{-j\omega_d(t-\tau)} \quad (12)$$

$$\text{where } \omega_d = a\omega_0 = (1-s)\omega_0 \quad (13)$$

The above expression indicates that for small scale factors, a Doppler shift can approximate the effect of scaling.

3.1 Compensating for RTC with Doppler shifts

Observe that the form of the companded narrow band signal closely resembles the kernel of the cross-ambiguity function. Hence, the cross-ambiguity function is well suited to correct for the ‘‘shift’’ introduced due to relative companding. [8, 12] present several techniques of using cross-ambiguity functions (CAFs) for determining the relevant delay and scale parameters.

For our case, the ratio of the sampling frequencies of the two signals, s , is always known: the sampling frequency of the template is known *a priori*, and can in fact be accurately controlled through correct construction. The instantaneous sampling frequency for the data obtained at a sensor may be estimated using several introspection algorithms. Also, the center frequency of the transmitted signal may be known *a priori* by construction. For arbitrary signals, it may also be estimated as the mean frequency as defined in [12, 13] by

$$\omega_0 = \frac{\int_{-\infty}^{\infty} \omega F(\omega) d\omega}{\int_{-\infty}^{\infty} F(\omega) d\omega} \quad (14)$$

To estimate the TOA, a generalized cross correlator (GCC) may be used on the RTC compensated signals. As before, if $f(t)$ represents the template and $g(t)$ the received signal, then we create a new signal, $f_1(t)$ which is a frequency shifted version of the template to

compensate for the current operating frequency of the sensor.

$$f_1(t) = f(t)e^{-j\omega_d t} \quad (15)$$

Signals $f_1(t)$ and $g(t)$ are then fed through matched filter to obtain an estimate for the time delay, τ .

$$\tau = \arg \max \left| \int_{-\infty}^{\infty} f_1(u)g^*(u+t)du \right| \quad (16)$$

$$\tau = \arg \max \left| \int_{-\infty}^{\infty} f(u)g^*(u+t)e^{-j\omega_d t} du \right| \quad (17)$$

The above expression may be viewed as a cross-ambiguity function evaluated at a given shift ω_d . This circumvents the need to compute several CAFs for differing values of scale and delay.

4. Implementation issues in Doppler RTC correction

The Doppler shift technique compensates for RTC by modulating the template signal with a complex exponential as shown in (15). Usually, the complex exponential is computed using Euler’s expansion:

$$\exp(j\omega_d t) = \cos(\omega_d t) + j \sin(\omega_d t) \quad (18)$$

For a discrete time system, the above evaluation must be performed for each sampling instant. Given a template of length N , this produces an $N \times 1$ vector of samples of the modulating complex exponential

$$\mathbf{e} = \cos(\omega_d \mathbf{t}) + j \sin(\omega_d \mathbf{t}) \quad (19)$$

where, $\mathbf{t}[k] = k / \omega_s$ is the vector of sampling instants, with $0 \leq k \leq N, k \in \mathbb{Z}$ and sampling frequency ω_s . Computing the elements of this complex exponential in terms of trigonometric functions is both computationally and temporally intensive. Furthermore, once the vector has been computed, its application to the real template vector requires N complex multiplications. Examining the structure and nature of this calculation and applying a few engineering assumptions, we can significantly reduce this burden.

For values of s fairly close to 1, or equivalently, when a is fairly small and when the period over which the Doppler correction must be employed is limited (If it is large, then the time-bandwidth product condition for narrow band signals is violated, making the Doppler shift assumption invalid), the product $\omega_d t$ is fairly small. Thus, we can make the following approximations $\cos(\theta) \approx 1$ and $\sin(\theta) \approx \theta$ (20)

$$\exp(j\omega_d t) = 1 + j(\omega_d t) \quad (21)$$

Expressing this as a vector of discrete samples, we have

$$\mathbf{e}[k] = 1 + j\omega_d \mathbf{t}[k] \quad (22)$$

This computation represents enormous savings in creating the correction vector, \mathbf{e} . The structure of each $\mathbf{e}[k]$ also enables us to apply the correction efficiently. The Doppler shifting of the template may be accomplished in a single pass, leading to an O(N) computation routine.

5. Alternative time shift based correction

The Doppler correction method compensates for relative companding by approximating the frequency scaling by a frequency shift: the modulation of the template sequence by a complex exponential shifts the spectrum of the template is to approximately line up with that of the scaled signal.

The Doppler correction has the advantage of offering a very intuitive and simple technique of compensating for the different sampling frequency between the nodes and the templates. While it also obviates the need to evaluate the passive ambiguity function for a large number of scales and shifts, it still suffers from a computational perspective.

As explained earlier, the sensor nodes are constrained in memory and computational power. In particular, the TI C67x DSPs used to provide the signal processing capabilities have a limited internal cache. When implementing computationally and temporally intensive operations such as a GCC, it is imperative that the memory access requirements be controlled to meet hard real-time constraints. Ensuring that the data and result vectors fit in the fast internal memory is a proven and routinely employed technique [14].

Both the Doppler correction and approximation techniques suffer in this regard because they convert normally real data vectors into complex vectors, doubling the initial memory requirement and causing performance to degrade. For e.g., an 8K point real-FFT takes a significantly lesser time than a complex-FFT of the same length.

The performance loss accrued over several iterations can mean the failure of a real-time constraint. Such a situation can occur in the computation of the cross spectral density (CSD) [15] of the received signal with the template.

Let us examine the relative companding problem again. As before, let

$$g(t) = f(s(t - \tau)) \quad (23)$$

where, $g(t)$, $f(t)$ are, respectively, the received and template signals, s is the scaling factor and τ is the time delay introduced.

The equations below recall the matched filtering operation.

$$R_{gf}(u) = \int_{-\infty}^{\infty} g(t)f(t+u)dt \quad (24)$$

$$\tau = \arg \max \left| \int_{-\infty}^{\infty} g(t)f(t+u)dt \right| \quad (25)$$

when $s = 1$, a value of $t = \tau$ maximizes R_{gf} . For the present case ($s \sim 1$, and narrow band signals), the value of t over a period (T_1, T_2) that maximizes R is given by,

$$\tau_m(T_1, T_2, t) = \arg \max \left| \int_{T_1}^{T_2} f(st - s\tau)f^*(t+u)dt \right| \quad (26a)$$

$$\tau_m(T_1, T_2, t) = u, \exists s(t - \tau) = (u + t) \quad (26b)$$

$$\therefore \tau_m(T_1, T_2, t) = (s - 1)t - s\tau \quad (26c)$$

Notice that this delay $\tau_m(T_1, T_2, t)$ is not fixed as in the previous case, but is ‘‘smeared’’ in time.

We wish to approximate this time varying delay $\tau_m(T_1, T_2, t)$ by a constant $\tau_d(T_1, T_2)$ chosen according to a least squared error criterion. Let the sum of the squared errors, $\epsilon(\tau)$, be given by

$$\epsilon(\tau_d) = \int_{T_1}^{T_2} e^2(t)dt = \int_{T_1}^{T_2} (\tau_m(t) - \tau_d)^2 dt \quad (27)$$

where (T_1, T_2) is the interval over which the two sequences are compared. Using the Leibniz integral rule [16], we have

$$\frac{\partial}{\partial \tau_d} \epsilon(\tau_d) = \int_{T_1}^{T_2} \frac{\partial}{\partial \tau_d} (\tau_m(t) - \tau_d)^2 dt + \quad (28)$$

$$(\tau_m(T_1) - \tau_d)^2 \frac{\partial}{\partial \tau_d} (T_1) - (\tau_m(T_2) - \tau_d)^2 \frac{\partial}{\partial \tau_d} (T_2)$$

For τ_d^o , the desired optimal value, the LHS of (28) vanishes.

$$\therefore \tau_d^o = \frac{1}{T_2 - T_1} \int_{T_1}^{T_2} \tau_m(t)dt = (s - 1) \frac{T_2 - T_1}{2} - s\tau \quad (29)$$

Over a given interval $[T_1, T_2]$, the effects of relative companding between $f(t)$ and $g(t)$ may be minimized in the least squares sense by constructing a time-shifted version of $f(t)$, denoted $\tilde{f}(t)$, as

$$\tilde{f}(t) = f(t + \tau_d) = f\left(t + (s-1)\frac{T_2 - T_1}{2} - s\tau\right) \quad (30)$$

In the discrete domain, the above equation may be expressed as

$$\tilde{f}[n] = \tilde{f}\left(\frac{2\pi n}{\omega_s}\right) = f\left(\frac{2\pi n}{\omega_s} + (s-1)\frac{T}{2} - s\tau\right), \quad (31)$$

where ω_s is the angular sampling frequency of f .

The analog signal $f(t)$ is usually not available to permit arbitrary time-shifting of the template signal. \tilde{f} would then need to be evaluated by interpolating at “arbitrary” time instants. While this is achievable, the interpolation in the time domain usually comes with a computationally expensive price tag.

An easier alternative may be found by migrating to the frequency domain. Taking the Fourier transform of the preceding equation, we obtain

$$\tilde{F}(\omega) = F(\omega)e^{j\tau_d\omega} \quad (32)$$

where $F(\omega) = \int_{-\infty}^{\infty} f(t)e^{-j\omega t} dt$ is the Fourier transform

of $f(t)$. Also note that we have dropped the superscript of τ_d in favor of brevity. As with the Doppler correction, it can be argued that the nature of τ_d and ω allow the correction factor $e^{j\tau_d\omega}$ to be computed as an approximation

$$e^{j\tau_d\omega} = 1 + j\tau_d\omega \quad (33)$$

The time-shift based approach has the following notable advantages

1. Smaller memory foot print for $F(\omega)$ computation and reduced memory latency: For real signals, the Fourier transform exhibits Hermitian symmetry. This may be exploited to reduce the number of computations required to compute the entire FFT. It also means that the input vector to the FFT routine is a real-vector, requiring half as much memory as its complex counterpart, reducing memory access times.
2. Ability to precompute $F(\omega)$: since the template is known by design, $F(\omega)$ may be computed offline. This obviates its computation at run-time entirely. This introduces huge savings in computation time.
3. Facility to efficiently implement correction in the frequency domain: As with the Doppler shift correction, we can utilize the nature of the correction to devise an efficient method of applying the correction in the frequency domain. This has the added advantage of allowing an *in situ* computation, bringing further reduction in memory access latencies and computation time.

6. Experimental Results

The figure 2 shows the schematic setup on which these algorithms were implemented and tested. The sensor nodes consisted of an FRS receiver connected to the relevant electronics. A “global” clock was derived using GPS signals one pulse per second (PPS) signals. The GPS signals were filtered and processed to reduce the effects of any timing jitters.

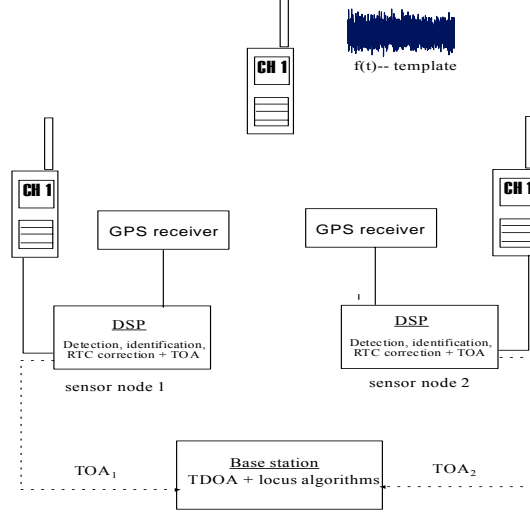


Figure 2. Schematic test setup. A FRS radio transmits a pseudo random sequence containing the template. The two nodes find the template and send TOA estimates to the remote base station

A 1-sec, 5 kHz band-limited pseudo-random sequence served as the template. A signal source placed at a controlled distance from both receivers transmitted a sequence containing the template. The sensor nodes had on-board a pre-manufactured version of the template. The detection and TOA operations were performed locally on the nodes and the TOA estimates were transferred to a PC (base-station) containing the TDOA location determining algorithms. The nominal sampling frequency at all the nodes was 480 kHz.

We present the results of the various experiments in Figure 3-5 and Table 1.

7. Conclusion

The availability of powerful low cost embedded DSPs with an impetus in wireless communications has led to a very large interest in developing self-contained distributed geolocation systems. On such systems, location estimates using TDOA techniques suffer due to inconsistencies in manufacturing and operating conditions. We have presented for low bandwidth, highly resource constrained real-time embedded systems, the related techniques of Doppler frequency

and time shifting to compensate for the adverse effects of different sampling frequencies on TOA/TDOA estimates. While the Doppler shift correction is found to be more accurate, the time-shift technique is more lucrative from a performance perspective.

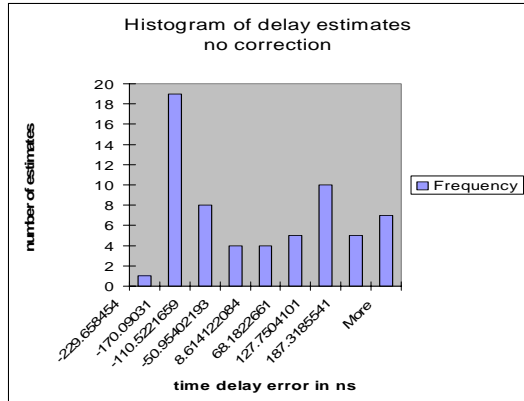


Figure 3 histogram of error in TDOA estimates without any correction applied

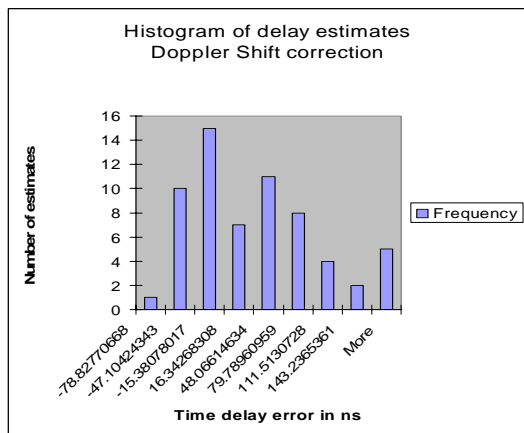


Figure 4 Histogram of errors in TDOA estimates with Doppler shift correction

References

1. Warrior, J et al; “They know where you are”; IEE. Spectrum, Vol.40, no.7, Jul 2003; pp. 20- 25
2. Kumar, S., Shepherd, D.; “SensIT: Sensor information technology for the war fighter”; Proc. Inter. Conf. on Information Fusion, Vol. 1, 2001
3. Bahl, P et. al.; “RADAR: an in-building RF-based user location and tracking system”, INFOCOM 2000, 19th Ann. Jt. Conf. IEEE Comp. and Com. Soc. Proc. IEEE, Vol.2, 2000, pp. 775-784
4. Drane, C. et. al. “Positioning GSM telephones” IEE. Comm. Mag. Vol.36, Iss.4 Apr 1998 pp. 46-54, 59
5. Stotts, L.B.: Unattended ground sensor related technologies; an army perspective, Proc. SPIE. Vol. 4040. (2000) 2–10

Table 1 Mean and standard deviation of errors in TDOA estimates

Correction type	Mean error (n sec)	Std dev. (n sec)
None	-30.57	153.85
Doppler shift	17.18	69.46
Time Shift	29.48	60.05

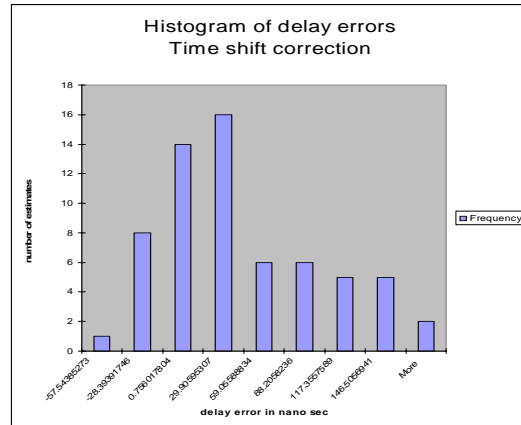


Figure 5 Histogram of errors in TDOA estimate when time-shift correction is used

6. Knapp, C., Carter, G.; “The generalized correlation method for estimation of time delay”; IEE. Trans. Acous., Speech, Sig. Proc. Vol.24, Aug 1976 pp. 320- 327
7. Proakis J; Manolakis, D; “Digital Signal Processing, Principles Algorithms, and Applications”, Prentice Hall, Third Ed., 1996.
8. Betz, J.; “Effects of uncompensated relative time companding on a broad-band cross correlator” IEEE Trans. Acous., Speech, Sig. Proc, Vol.33, Jun 1985
9. Remley, W.; “Correlation of signals having linear delay”, Acoust. SOC. Amer., vol. 35, pp. 65-69, Jan. 1963.
10. W. B. Adams et al.; “Correlator compensation requirements for passive time delay estimation with moving source or receivers”; IEE. Trans. Acoust., Speech, Signal Processing, vol. 28, pp.158-168, Apr. 1980.
11. Weiss, L.G.; “Wavelets and wideband correlation processing”, IEE. Sig Proc Mag Vol.11, Jan 1994 pp13-32
12. Stein, S; “Algorithms for Ambiguity function processing”; IEE. Trans Acou., Spch. & Sig. Proc. Vol.29, Iss.3, Jun 1981 pp 588- 599
13. Ulman, R.; Geraniotis, E; “Wideband TDOA FDOA processing using summation of short-time CAF’s”, IEE. Trans. Sig. Proc. Vol.47, no 12, Dec 99
14. Dharia A. et al; “Signal Processing Examples Using the TMS320C67x Dig. Sig. Proc. Library (DSPLIB)”, Texas Instruments, App. Rpt SPRA947

15. Welch, P.; "A method based on time averaging over short, modified periodograms"; IEEE Trans. on Audio and Electro., Vol.15, Iss.2, Jun '67 pp. 70- 73
16. Leibniz Integral Rule, mathworld.wolfram.com